



Cite this: *New J. Chem.*, 2019, 43, 874

Pyrazoline-based colorimetric and fluorescent probe for detection of sulphite†

Tomasz Uchacz,^a Gabriela Jajko,^a Andrzej Danel,^{*b} Paweł Szlachcic^b and Szczepan Zapotoczny^a

Two pyrazoline-based fluorescent and colorimetric probes have been synthesized and their photo-physical properties have been investigated by means of electronic absorption and emission spectroscopy. The compounds differ from each other by the presence of a phenyl or thiophene end group attached to the α,β -unsaturated ketone. The probes detect sulphite anions in the Michael addition reaction to the α,β -unsaturated ketone with a high selectivity and good sensitivity (7.56 μM for phenyl and 4.87 μM for the thiophene counterpart). Here, the optical response is based on the recovery of triphenylpyrazoline fluorescence, which is largely blue-shifted as compared to weak charge transfer emission of the sensors. This large hypsochromic shift of the emission maximum along with a strong fluorescence enhancement (up to $I^{\text{sulphite}}/I_0 = 43$) can be an advantage in terms of the accurate evaluation of the fluorescence intensity ratio. The pyrazoline-based sensor decorated with thiophene is able to detect sulphite species in river water solutions with a good selectivity and sensitivity.

Received 3rd October 2018,
Accepted 30th November 2018

DOI: 10.1039/c8nj05017a

rsc.li/njc

1. Introduction

Sulphur dioxide is a vital component of acid rain and smog, which is one of the main problems faced by citizens in the big metropolises. Acid rain contributes to destruction of monuments, while smog can affect the human respiratory system. In high doses gaseous sulphur dioxide is poisonous and there are records that it was used for deliberate poisoning of people.¹ Prolonged exposure to gaseous pollutants like SO_2 , NO_2 and CO can be a factor for acute stroke death.^{2,3} One of the main sources of SO_2 is combustion of fossil fuels like coal and petroleum. On the other hand, it should be remembered that volcanoes can release a huge amount of that gas into the atmosphere as well. By way of illustration, in 2014 the Holuhraun volcano (Iceland) emitted 1030 kilograms per second of sulphur dioxide during the first 3 months of the eruption, which obviously contributed to the deterioration of the health status of the Iceland population.⁴ SO_2 is a gas which exists in aqueous solution at neutral pH as an equilibrium between bisulphite and sulphite ions (NaHSO_3 and Na_2SO_3 , 1:1 M/M). Once SO_2 is inhaled into the human body and dissolved in body fluid, it will immediately induce its biological effects in the form of its derivatives. In addition, bisulphite/sulphite enters the body *via*

foods, beverages and drugs because sulphating agents (sulphur dioxide, metabisulphite, bisulphite and sulphite) are widely used as preservatives.⁵ In some cases it could be very dangerous for humans. Sulphite oxidase deficiency is a fatal disease that causes neurological disorders, mental retardation, physical deformities, degradation of the brain, and early death.^{6,7} Thus, the sulphite level in the body must normally be tightly maintained.

In recent years, growing interest in the application of fluorescent sensors towards various analytes like cations, anions and neutral molecules has been observed. Quite a lot of work was devoted to developing sensors for sulphite and bisulphite anions. Zhou *et al.* synthesized a fluorescent turn-on probe based on 4-hydrazinyl-1,8-naphthalimide with a detection limit of 0.56 μM .⁸ A large quantity of fluorescent probes for SO_3^{2-} and HSO_3^- are based on a coumarine system. For example, Li *et al.* applied 3-formyl-7-*N,N*-diethylcoumarine for bioimaging of hydrogen sulphite. The non-emissive aldehyde ($\Phi = 0.02$) emitted green light ($\Phi = 0.43$) upon nucleophilic addition of hydrogen sulphite.⁹ Due to our interest in strongly emissive 1*H*-pyrazolo-[3,4-*b*]quinolines,^{10–13} we decided to exploit another pyrazole derivative, namely 1,3,5-triarylpyrazoline, as a potential fluorescent sensor for various analytes. This system was applied mainly for the detection of various cations. For example, Wang *et al.* synthesized 1-phenyl-3-(2-pyridyl)-5-phenylpyrazoline. The spectroscopic studies showed that this compound is a typical OFF-ON fluorescence sensor which exhibits high selectivity and affinity toward Zn(II) cations.¹⁴ A similar affinity was observed in the case of 1-(2-benzothiazole)-3-(2-thiophene)-2-pyrazoline.¹⁵ However, there are only a few examples of pyrazoline based sensors for

^a Faculty of Chemistry, Jagiellonian University, ul. Gronostajowa 2, 30-387 Kraków, Poland. E-mail: tomaszuchacz55@gmail.com

^b Institute of Chemistry, Department of Food Technology, Agricultural University, ul. Balicka 122, 31-149 Kraków, Poland. E-mail: rrdanela@cyf-kr.edu.pl

† Electronic supplementary information (ESI) available. See DOI: 10.1039/c8nj05017a

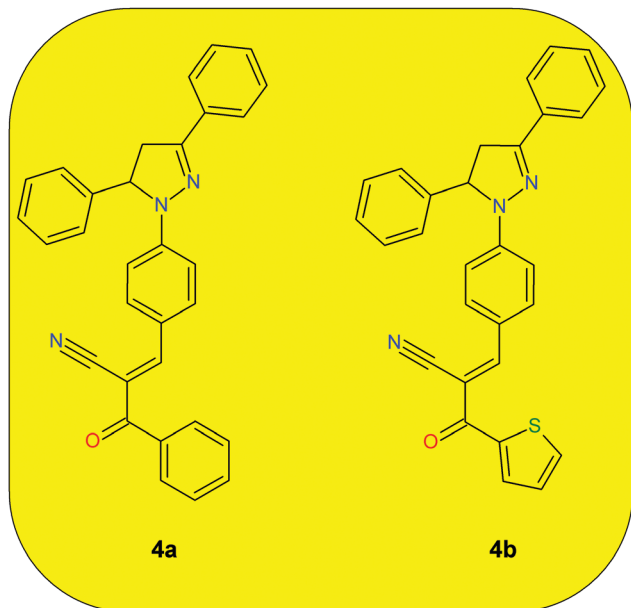


Fig. 1 Molecular structures of the investigated compounds.

thiol derivatives. For instance, Miao *et al.* synthesized a fluorescent probe based on coumarin and pyrazoline to detect cysteine in living cells with an appreciable limit of detection ($5.08 \mu\text{M}$).¹⁶ Another group investigated a pyrazoline-coumarin hybrid combined with a 2,4-dinitrobenzenesulfonyl (DNBS) moiety.¹⁷ In this case, the emission is recovered in the presence of thiols due to the release of the fluorescence quencher – DNBS. To the best of our knowledge pyrazoline based probes for the detection of sulphite ions have not been investigated yet.

In this paper, two 1,3,5-triarylpyrazoline based sensors were presented (**4a** and **4b**) as doubly activated Michael addition type indicators for the colorimetric and ratiometric fluorescent detection of sulphite (see Fig. 1). The sensors exhibit high selectivity and sensitivity to SO_3^{2-} . Two different end groups were introduced to control the kinetics of analyte addition and the sensitivity to the sulphite anion. The advantage of the reported probes is their high optical response and relatively fast time response in the presence of small amounts of analyte (9–11 min in the presence of 45 equivalents) which is comparable with the majority of currently available Michael type indicators (5–60 min in the presence of 10–500 equivalents of sulphite).^{18–20} In addition, the compound decorated with thiophene was able to detect sulphite anions in river water samples.

2. Experimental

2.1. Materials and apparatus

All reagents were purchased from Sigma Aldrich or Alfa Aesar and used without further purification. The applied dimethylformamide (DMF) was of spectroscopic grade. The salts employed in stock solutions of sodium anions were: nitrate, nitrite, bromide, chloride, fluoride, iodide, acetate, thiocyanate, sulphate, sulphite, glutathione, cysteine, homocysteine, hydro-sulphide, bisulphite, and cyanide. ^1H NMR and ^{13}C NMR spectra

were carried out by means of a Bruker Avance III 600 spectrometer operating at 600 and 150 MHz, respectively, in CDCl_3 with TMS as an internal standard. Melting points were determined on a Mel-Temp Apparatus II (capillary), and they are uncorrected. FTIR spectra of the molecules were recorded in the range of $4000\text{--}500 \text{ cm}^{-1}$ at resolution of 4 cm^{-1} using a MATTSON 3000 FT-IR (Madison, Wisconsin, USA) spectrophotometer. MS analysis was carried out by the ESI-MS-TOF method.

2.2. Photophysical and electrochemical measurements

Fluorescence quantum yield and fluorescence lifetime measurements were carried on the deaerated solutions (by saturation with argon) and the sample concentration was *ca.* $2.8 \mu\text{M}$. UV-vis electronic absorption spectra were recorded using a Varian Cary Eclipse spectrometer and the emission spectra (with the correction for spectral sensitivity) were measured by Fluorolog-tau3 equipped with time-correlated single photon counting apparatus (diode laser N-455, IBH-UK). Deconvolution analysis of the decay curves yielded the corresponding fluorescence lifetimes. For this purpose, the instrument-response function was recorded by using a light-scattering Ludox solution. The fluorescence quantum yield measurements were estimated with reference to fluorescein in 0.1 M NaOH aqueous solution ($\Phi_{\text{fl}} = 0.92$).²¹

Differential pulse voltammograms of the studied compounds were measured with a PalmSens3 potentiostat. One platinum wire ($\varnothing = 0.5 \text{ mm}$), platinum coil ($\varnothing = 3.0 \text{ mm}$) and gold wire ($\varnothing = 0.5 \text{ mm}$) were used as a counter, working and quasi-reference electrode, respectively. The potential of the quasi-reference electrode was calibrated using the ferrocene/ferrocenium couple as an internal standard. The solution of the sensor ($\sim 0.5 \text{ mM}$) was prepared in a suitable electrolyte ($\sim 50 \text{ mM}$ solution of $\text{Bu}_4\text{N}^+\text{ClO}_4^-$ in DMF). Prior to the measurements the solutions were purged with argon to remove residual oxygen.

2.3. Procedure of anion sensing

The absorption and fluorescence titration experiments were carried out on non-degassed samples by adding a suitable amount of titrant to a quartz cuvette containing 2 ml of the dye at a concentration of $\sim 2.8 \mu\text{M}$ (1:1 deionised water or Hepes buffer/dimethylformamide solution). Measurements were carried out in 1 cm cuvettes after 15 min stabilization at room temperature. The excitation wavelengths for the fluorescence measurements on the addition of sodium salt were chosen to agree with the isosbestic points of the UV/vis absorption titration spectra: $\lambda_{\text{ex}} = 403 \text{ nm}$ for **4a**, $\lambda_{\text{ex}} = 407 \text{ nm}$ for **4b**.

The Michael addition reaction kinetics was investigated in the presence of 45 equivalents of sulphite. The analysis was carried out by monitoring the fluorescence changes at 587 nm (**4a**) and 605 nm (**4b**), which correspond to the maximum of the emission band of the substrate. As the excitation wavelength, 479 nm for **4a** and 496 nm (**4b**) was chosen. In order to avoid the oxygen-sulphite reaction, the measurements were conducted on deaerated solutions (1:1 Hepes buffer (pH = 8)/DMF).

The determination of sulphite in river water samples was carried out by the addition of an appropriate amount of sulphite into a 1 : 1 Hepes buffer (pH = 8)/DMF mixture. The absorption and emission spectra were measured after 30 minutes of equilibration.

The limit of detection (LOD) was determined by the analysis of the fluorescence intensity changes at 460 nm (for both studied compounds), induced by the presence of analyte. The detection limit was calculated using the following equation:

$$\text{LOD} = \frac{3.3 \cdot s}{b} \quad (1)$$

where: s – standard deviation of low concentration, b – slope of calibration line.

2.4. Synthesis of compounds 4b and 4a

The presented pyrazoline derivatives (4) were prepared according to the synthetic procedure illustrated in Scheme 1. The starting 1,3,5-triphenylpyrazoline 2 was synthesized from chalcone 1 reacted with phenylhydrazine hydrochloride in sodium acetate/acetic acid solution under ultrasound irradiation.²² Pyrazoline 2 was formylated with POCl₃/DMF yielding aldehyde 3.²³ Arylacetonitriles (3-oxo-3-phenylpropanenitrile and 3-oxo-3-(thiophen-2-yl)propanenitrile) were prepared according to the literature protocol from acetonitrile and corresponding ester: methyl benzoate or thiophene-2-carboxylic acid methyl ester, respectively.²⁴ Finally, aldehyde 3 and the corresponding nitrile were reacted together in the presence of piperidine under ultrasound irradiation. The reaction was finished within two hours.

(E)-2-Benzoyl-3-[4-(3,5-diphenyl-3,4-dihydropyrazol-2-yl)phenyl]prop-2-enitrile (4a). Aldehyde 3 (163 mg, 0.5 mmol) and 3-oxo-3-phenylpropanenitrile (108 mg, 0.75 mmol) were dissolved in 96% ethanol (10 mL) in a 25 mL round-bottomed flask. To the mixture 3 drops of piperidine were added and the reaction mixture was irradiated in the water bath of a laboratory ultrasonic cleaner for two hours. After finishing, the precipitate was filtered off and crystallized from toluene.

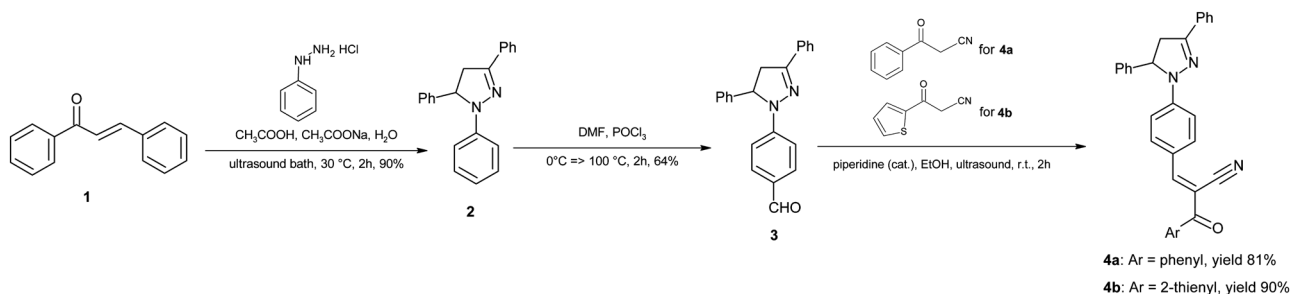
Yellow crystals, 200 mg, 81%, mp. 178–180 °C (toluene). ¹H NMR (600 Hz, CDCl₃, δ/ppm, Fig. S1, top, ESI⁺): 7.96 (s, 1H_{vinyl}); 7.93 (d, J = 9.2 Hz, 2H), 7.82–7.81 (m, 2H), 7.77–7.75 (m, 2H), 7.58–7.55 (m, 1H), 7.48–7.46 (m, 2H), 7.42–7.40 (m, 3H), 7.37–7.34 (m, 2H), 7.31–7.28 (m, 1H), 7.26–7.24 (m, 2H), 7.12 (d, J = 8.2 Hz, 2H), 5.44 (dd, J = 12.1, 5.4 Hz,

1H_{pyrazoline ring H4a}), 3.93 (dd, J = 12.1, 17.3 Hz, 1H_{pyrazoline ring H3}), 3.25 (dd, J = 17.3, 5.4 Hz, 1H_{pyrazoline ring H4b}). ¹³C NMR (150 Hz, CDCl₃, δ/ppm, Fig. S1, bottom, ESI⁺): 189.9, 155.5, 151.1, 147.9, 140.9, 137.1, 134.1, 132.5, 131.6, 129.9, 129.5, 129.0, 128.8, 128.4, 128.2, 126.3, 125.5, 122.3, 118.8, 113.2, 103.0, 63.3, 43.6. IR (KBr): ν_{max} 2206 (C≡N), 1652 (C=O) cm⁻¹. MS (ESI, m/z (%), Fig. S2, ESI⁺): 476(100) [M + Na⁺], 360(13), 297(63), 178(9), 116(9), 105(33). HRMS (ESI): m/z calc. for C₃₁H₂₃N₃O: 453.1841; found 476.1732 [M + Na⁺]⁺. Anal. calcd for C₃₁H₂₃N₃O: C, 82.10; H, 5.11; N, 9.26. Found: C, 81.60; H, 5.05; N, 9.09.

(E)-3-[4-(3,5-Diphenyl-3,4-dihydropyrazol-2-yl)phenyl]-2-(thiophene-2-carbonyl)prop-2-enitrile (4b). This compound was prepared in the same way as 4a *i.e.* from aldehyde 4 (160 mg, 0.5 mmol) and 3-oxo-3-(thiophen-2-yl)propanenitrile (115 mg, 0.75 mmol). Red crystals, 200 mg, 90%, mp. 246.8 °C (toluene). ¹H NMR (600 Hz, CDCl₃, δ/ppm, Fig. S3, top, ESI⁺): 8.25 (dd, J = 3.9, 1.0 Hz, 1H_{thiophene ring H3}), 8.18 (s, 1H, H_{vinyl}), 7.97 (d, J = 9.2 Hz, 2H), 7.78–7.76 (m, 2H), 7.69 (dd, J = 5.0, 1.0 Hz, 1H_{thiophene ring H5}), 7.46–7.40 (m, 3H), 7.38–7.35 (m, 2H), 7.32–7.30 (m, 1H), 7.27–7.25 (m, 2H), 7.16 (dd, J = 5.0, 3.9 Hz, 1H_{thiophene ring H4}), 7.13 (d, J = 8.9 Hz, 2H), 5.45 (dd, J = 12.0, 5.3 Hz, 1H_{pyrazoline ring H4a}), 3.94 (dd, J = 17.4, 12.1 Hz, 1H_{pyrazoline ring H3}), 3.26 (dd, J = 17.4, 5.4 Hz, 1H_{pyrazoline ring H4b}). ¹³C NMR (150 Hz, CDCl₃, δ/ppm, Fig. S3, bottom, ESI⁺): 178.9, 155.8, 151.3, 148.0, 143.1, 141.0, 134.6, 134.4, 133.8, 131.8, 130.0, 129.7, 128.9, 128.5, 128.4, 126.5, 125.7, 122.7, 119.8, 113.4, 101.0, 63.5, 43.7. IR (KBr): ν_{max} 2203 (C≡N), 1605 (C=O) cm⁻¹. MS (ESI, m/z (%), Fig. S4, ESI⁺): 482(100) [M + Na⁺], 297(21). HRMS (ESI): m/z calc. for C₂₉H₂₁N₃OS: 459.1405; found 482.1298 [M + Na⁺]⁺. Anal. calcd for C₂₉H₂₁N₃OS: C, 75.79; H, 4.61; N, 9.14; S 6.98. Found: C, 75.86; H, 4.62; N, 8.92; S 6.85.

2.5. DFT calculations

Gaussian09 was used for DFT (density functional theory)^{25,26} calculations.²⁷ The ground-state structures of molecules were optimized using the B3LYP method^{28,29} with the cc-pVDZ standard basis set. The optimized structures of the sensors (and adducts with sulphite) can be found in Fig. S5–S8, ESI⁺. The real energy minima of the optimized structures have been checked by calculation of the Hessian matrix and verification of the absence of imaginary frequencies. With the aid of the TD-B3LYP/cc-pVDZ method the vertical excited-state energies of the dyes and analyte-dye products were estimated as well.



Scheme 1 Synthesis route leading to (E)-2-benzoyl-3-[4-(3,5-diphenyl-3,4-dihydropyrazol-2-yl)phenyl]prop-2-enitrile (4a) and (E)-3-[4-(3,5-diphenyl-3,4-dihydropyrazol-2-yl)phenyl]-2-(thiophene-2-carbonyl)prop-2-enitrile (4b).

The Polarisable Continuum Model (PCM)^{30,31} was employed to simulate the influence of DMF polarity.

3. Results and discussion

3.1. Photophysical and electrochemical properties of **4a** and **4b**

Room temperature absorption and emission spectra of **4a** and **4b** in DMF are presented in Fig. 2 and some basic photophysical and electrochemical parameters are listed in Table 1. Both compounds are characterized by a strong absorption ($\epsilon_{\text{abs}} = 45\,000\text{ M}^{-1}\text{ cm}^{-1}$) covering the range from 550 nm to 400 nm. The maximum of absorption for **4a** was located at 469 nm, while for **4b** it was 10 nm bathochromically shifted. The same trend was observed in fluorescence but the shift was slightly larger (18 nm). Both compounds displayed weak fluorescence and short fluorescence lifetimes. The calculated constant rates of nonradiative deactivation were found to be two orders of magnitude larger than radiative ones. A closer look at the molecular structure of the investigated molecules shows that this effect may be associated with free motions (rotations) of the ethylenecyanocarbonyl group, *trans-cis* photoisomerisation or a radiationless back electron transfer process. However, a Gaussian-like, broad absorption band and a large Stokes-shift indicate the existence of the charge transfer emitting state. In addition, the process is feasible from the thermodynamic point of view. The calculated Gibbs energy of intramolecular charge transfer (ICT) is strongly negative (see Table 1). Therefore, it seems

that all of the above-mentioned processes may contribute to the deactivation pathway of the excited state of the molecules studied. However, a definite answer to the question requires a deep analysis of photophysical processes (*e.g.* solvatochromism) which will be carried out in our laboratory with a subsequent report in due course.

Analyzing the results from electrochemical measurements (Table 1), one can notice that the reduction potential of **4b** is slightly decreased as compared to **4a**. This is somewhat expected if we consider the fact that the acceptor properties of thiophene are better than that of benzene (-1.84 V and -2.56 V – estimated by addition of energy gap to the oxidation potential of thiophene or benzene, respectively³²). Surprisingly, it does not improve the exothermicity of the photoinduced electron transfer process because the thiophene simultaneously deteriorates the oxidation properties of the probe.

To apply the studied compounds in environmental or medical studies, the impact of water on the absorption and emission spectra of the dyes was also explored. In our further experiments, we decided to use a 1:1 water/DMF solvent mixture as a good compromise between the solubility of the sensor and analyte, in particular, sulphite anions. In both cases, the maximum of absorption is red-shifted by about 12 nm (emission spectrum: 12 nm for **4a** and **4b**, respectively) as compared to DMF solution. This bathochromic shift may be explained in terms of the energy stabilization of the molecule induced by highly polar solvent (water). Moreover, the changes in the colour of absorption/emission were accompanied by a fluorescence intensity reduction ($\Phi_{\text{fl}} = 0.006$ and $\Phi_{\text{fl}} = 0.007$ for **4b** and **4a**, respectively).

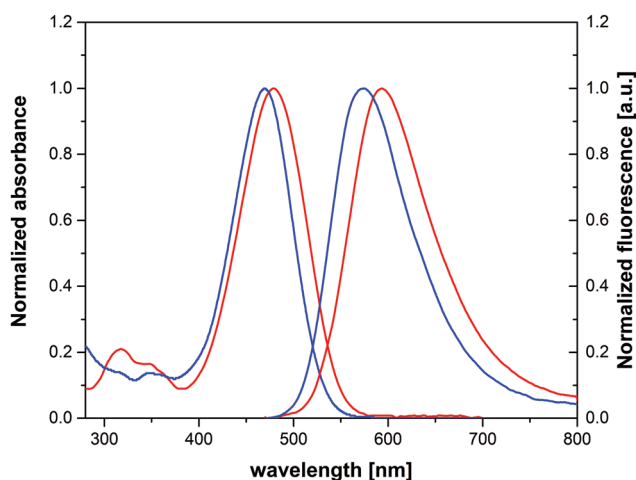


Fig. 2 Electronic absorption and emission spectra of **4a** (blue line) and **4b** (red line) recorded in DMF solution.

3.2. Anion recognition

Probes contained an α,β -unsaturated carbonyl system usually detect anions in the Michael addition of a nucleophile to the activated double bond system. The presented probes are composed of a triphenylpyrazoline fluorophore and an ethylenecyanocarbonyl group ended with thiophene or phenyl. It is expected that anions can be added to the β -position of the doubly activated Michael acceptor to generate the stabilized anionic species. In order to explore the selectivity of the sensors to sulphite, absorption and emission spectra were recorded in the presence of 45 equivalents of different anions: nitrate, nitrite, bromide, chloride, fluoride, iodide, acetate, thiocyanate, sulphate, sulphite, glutathione, cysteine, homocysteine, hydro-sulphide, bisulphite and cyanide. As shown in Fig. 3, the investigated probes are sensitive to sulphite. Upon addition of

Table 1 Photophysical and electrochemical parameters of the investigated dyes dissolved in DMF. The Gibbs energy of the photoinduced electron transfer process was calculated according to the following equation: $\Delta G_{\text{et}} = E_{\text{ox}} - E_{\text{red}} - E_{00} + C$; C – the Coulomb term was taken as -0.056 eV . Redox potentials were obtained from the position of the first oxidation/reduction peak and the DPV voltammograms can be found in the ESI (Fig. S9 and S10). λ_{abs} corresponds to the maximum of the lowest energy absorption band, E_{00} – energy gap between the HOMO and LUMO energy levels estimated from the onset of the lowest energy absorption band

Compound	λ_{abs} [nm]	ϵ_{abs} [$\text{M}^{-1}\text{ cm}^{-1}$]	λ_{flu} [nm]	Φ_{flu}	τ_{flu} [ns]	k_{nr} [10^7 s^{-1}]	E_{ox} [V]	E_{red} [V]	E_{00} [eV]	ΔG_{et} [eV]
4a	469	47 090	575	0.014	0.18	7.78	0.679	-1.349	2.353	-0.381
4b	479	43 496	593	0.016	0.20	8.00	0.713	-1.273	2.275	-0.345

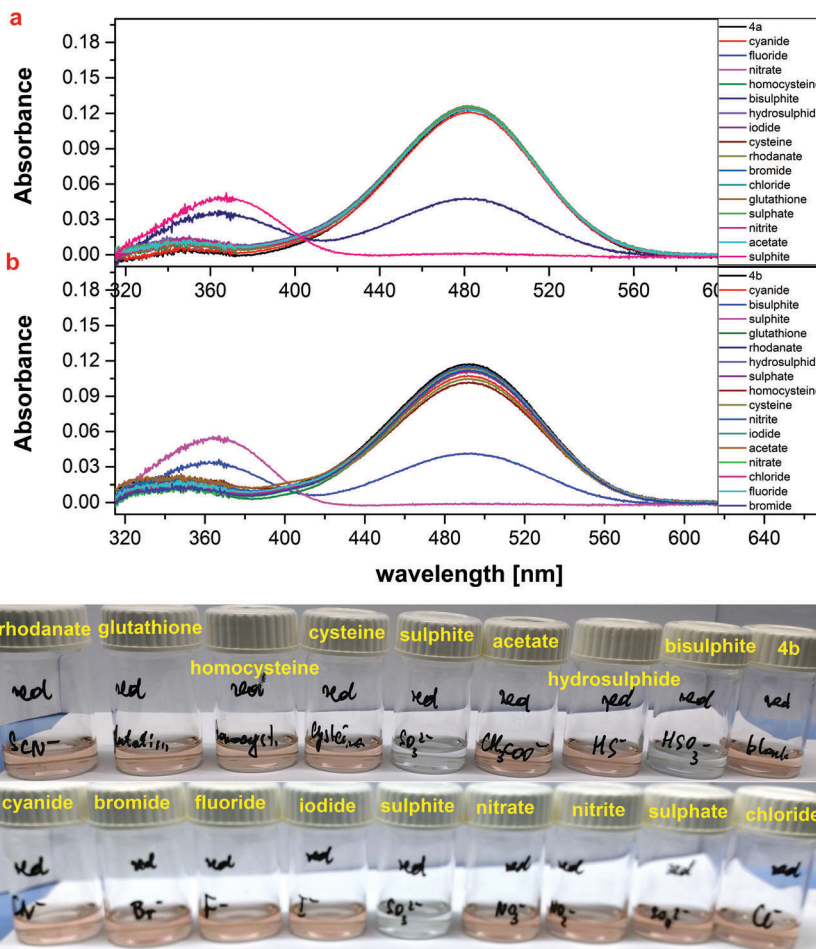


Fig. 3 Absorption spectra of **4a** (a) and **4b** (b) in the presence of 45 equivalents of different anions. The bottom picture illustrates the colour change of **4b** upon addition of the anions under study.

sulphite to the solution of **4a** (**4b**), the absorbance at 481 nm (491 nm) was gradually decreased with a new band appearing at 370 nm. Simultaneously, a distinct colour change from orange to colourless was clearly observed (see Fig. 3 and Fig. S11, ESI[†]) indicating that the intermolecular charge transfer process is turned off due to the Michael addition of sulphite.

The newly formed band (at 370 nm) may be assigned to the excitation of 1,3,5-triphenylpyrazoline (parent molecule)³³ which is now electronically decoupled from the end group: phenyl or thiophene. In order to support this hypothesis, DFT calculations (in DMF) were performed and the values of vertical energy excitations are as follows: 520 nm (385 nm) for **4b** (**4b** + sulphite), 506 nm (386 nm) for **4a** (**4a** + sulphite). Certainly, the obtained values are slightly underestimated; nevertheless, they reflect a general trend in hypsochromism after the binding process of sulphite.

It is worth adding that at pH = 7.2 (pH of dionized water used) both of the studied probes can also interact with HSO_3^- , but the photophysical changes were less dramatic than in the presence of a sulphite anion. Hence, the observed differences in the absorption spectra of the sulphite and bisulphite adduct may point to a better selectivity of the investigated probes to

sulphite species (Fig. 3 and Fig. S11, ESI[†]). Therefore, a further analysis of the photophysical data involves only the interactions between the studied probes and sulphite anion.

3.3. Fluorescence response of compounds **4a** and **4b** towards SO_3^{2-}

Free compound **4a**, excited at the isosbestic point (407 nm), displays two main bands locating at 462 nm (some traces of the band) and 587 nm, which can be attributed to the emission from the locally excited state (LE) and intramolecular charge transfer state (ICT), respectively. The presence of sulphite leads to the disappearance of the ICT band and the appearance of a new band at 475 nm, which can be attributed to the emission of 1,3,5-triphenylpyrazoline.³³ The analysis of fluorescence changes at 475 nm showed that the observed emission enhancement is significant ($R_{4a} = I^{\text{sulphite}}/I_0 = 43$) (Fig. 4). Again, the experiment shows that the Michael addition reaction interrupts the π -conjugation leading to the recovery of triphenylpyrazoline emission. This statement is additionally supported by the studies of fluorescence excitation spectra of the substrate and product (Fig. S12 and S13, ESI[†]). The obtained spectra match well with the absorption spectra confirming that the emission

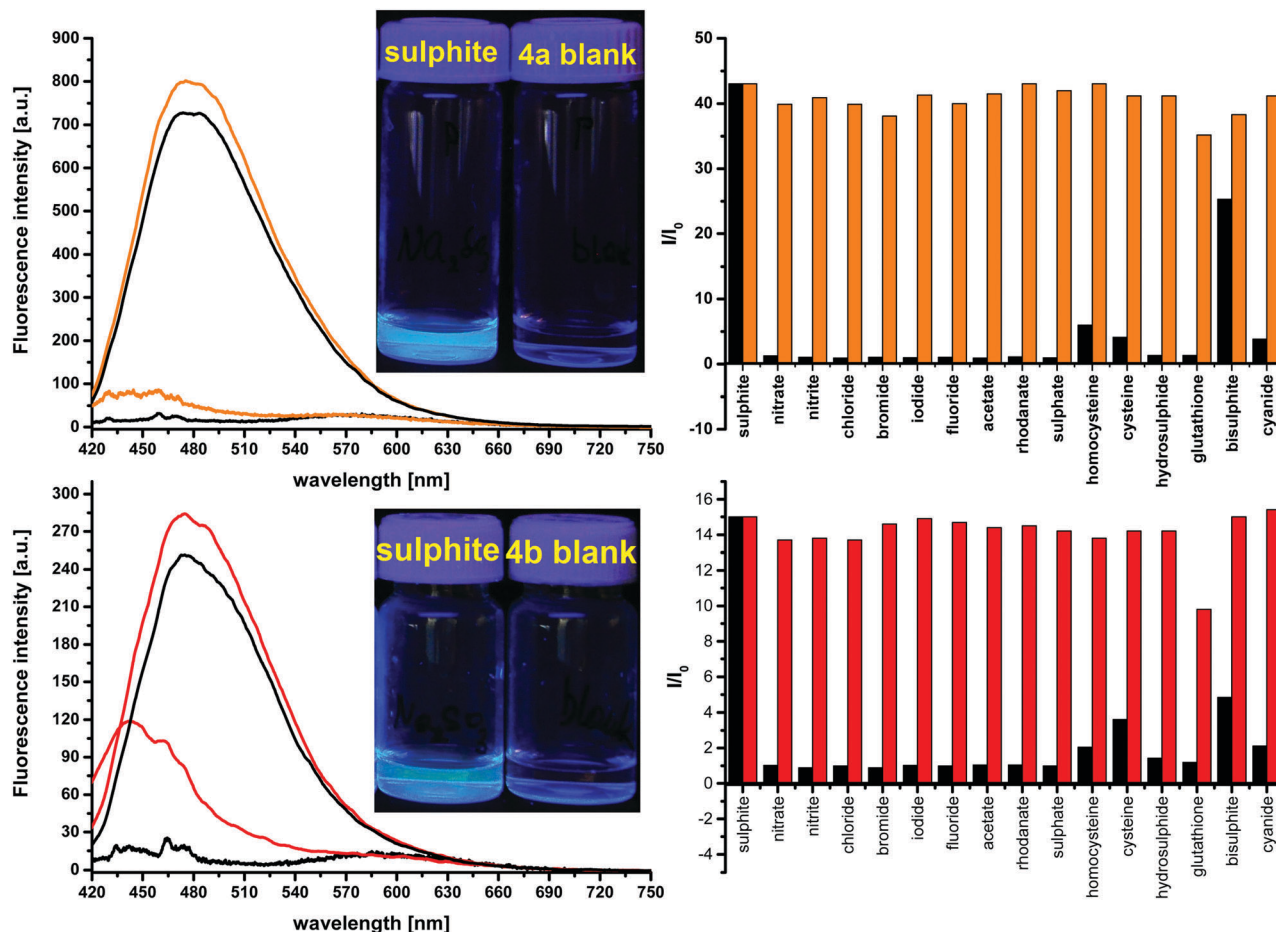


Fig. 4 Fluorescence changes induced by the Michael addition of sulphite anions. Top corresponds to **4a** and bottom to **4b**. Orange and red lines correspond to the HEPES/DMF mixture and black to water/DMF solution. Right black bars describe the enhancement of fluorescence induced by the presence of different anions recorded in water/DMF solution. Orange and red bars relate to the competition between sulphite and other anions.

at 475 nm originates from the locally excited state of the parent molecule.

It is worth noting that the difference in emission maxima (ICT and LE) before and after sulphite addition is very large $\Delta\lambda = 112$ nm which results in well separated fluorescence bands. In addition, due to the low intensity of the ICT emission band, the sensor can be considered as an OFF-ON fluorescence probe. These photophysical features can be an advantage in terms of accurate measurements of the intensities of the two emission peaks and, in consequence, a good evaluation of the fluorescence intensity ratio.

The photophysical behaviour of **4b** is very similar to that observed for **4a**. The product of Michael addition is characterized by blue-shifted emission with a maximum at 478 nm. Interestingly, the emission shift is higher ($\Delta\lambda = 127$ nm, see Fig. 4) as compared to probe **4a** confirming that the electron withdrawing effect is more pronounced in **4b** because of the presence of a slightly better acceptor. What distinguishes the investigated probes is their fluorescence intensity ratio in the presence and absence of sulphite. **4b** is characterized by lower maximal intensity and reduced fluorescence enhancement $R_{4b} = I^{\text{sulphite}}/I_0 = 15$ as compared to **4a**. The determined fluorescence quantum yields for **4a**-sulphite and **4b**-sulphite equal 0.28 and 0.15, respectively.

It is noteworthy that both values are lower as compared to 1,3,5-triphenylpyrazoline dissolved in protic methanol – $\Phi_n = 0.38$.³⁴ The quenching of pyrazolines' native fluorescence may be caused by photoinduced electron transfer occurring between the electronically decoupled thiophene/phenyl and 1,3,5-triphenylpyrazoline part. Obviously, the quenching process is more efficient in the **4b**-sulphite adduct due to the presence of a better electron donor/acceptor group – thiophene.

Fig. 4 (orange and red bars) presents also the influence of competitive anions on the selectivity of probes **4a** and **4b** for the detection of sulphite anions. Our studies revealed no effect of the second anion except for glutathione for which the fluorescence signal is reduced by 20% for **4a** (35% for **4b**). The analysis of the literature shows that glutathione can be converted to glutathione-S-sulphonate in a large excess of sulphite concentration.³⁵ Consequently, it is very likely that some part of sulphite may be bound to the glutathione resulting in reduced fluorescence signal.

3.4. The effect of pH on SO_3^{2-} recognition

The impact of pH on fluorescence spectra was studied in buffer mixed solutions (DMF/HEPES 1:1) and the results are presented in Fig. 5. The fluorescence intensity monitored at 475 nm slowly

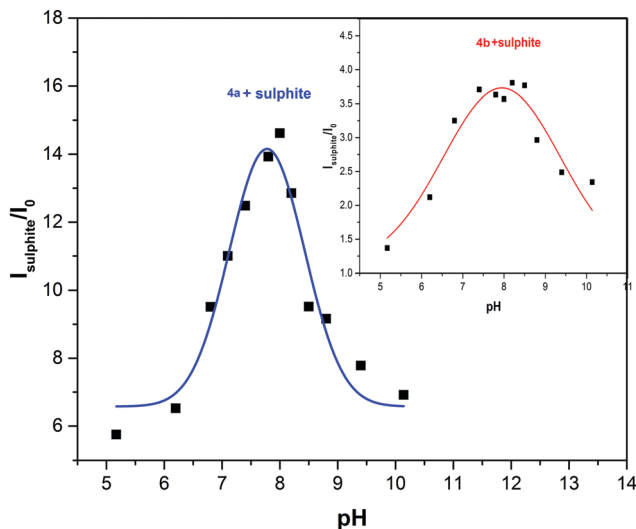


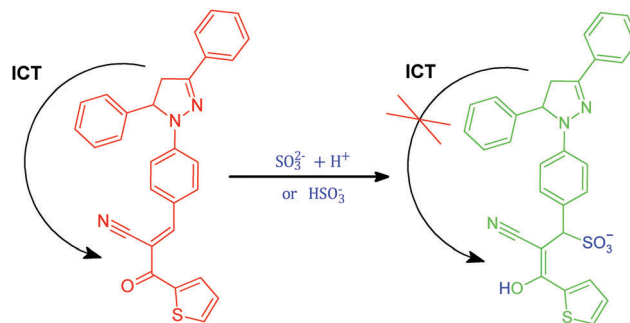
Fig. 5 Effect of pH on the fluorescence of the sulphite-**4a** product and sulphite free **4a** probe (inset) monitored at 475 nm.

but systematically increased over pH 5.0–10.00 (see inset Fig. S14 and S15, ESI[†]), but the fluorescence still had a dual character. This shows that the probes rather do not undergo Michael reaction with OH[−] and a higher concentration of OH[−] presumably leads to new charge relocation within the molecule which may promote an increased population of the locally excited state ($I_{4b}^{LE}/I_{4b}^{CT} = 10$, $I_{4a}^{LE}/I_{4a}^{CT} = 2.73$ while in water/DMF the ratio amounts to 1 in both cases). Our experiment also revealed that the best optical signal of product to optical signal of substrate ratio was at pH = 8 for both studied probes. Similar to water/DMF solution, the enhancement of fluorescence induced by a Michael addition product is larger for **4a** than **4b**.

Finally, it is noteworthy that pH has a negligible impact on the absorption of the free probes (see the Charts S16 and S17 in the ESI[†]) and, consequently, the observed effect arises from nucleophilic addition of sulphite.

3.5. Sensing mechanism

In order to confirm the nucleophilic addition by sulphite to the double bond system, the measurement of ¹H NMR spectra of the product (**4a**-sulphite adduct) in DMSO-*d*₆/D₂O was performed (1 mg, 2.2 μmol of **4a** was dissolved in 0.3 ml of DMSO-*d*₆ and a solution of 50 mg, 400 μmol of anhydrous Na₂SO₃ in 0.95 ml of D₂O was added). The ¹H NMR spectrum of the substrate exhibits a characteristic singlet signal at 7.96 corresponding to the vinyl proton which disappeared due to the nucleophilic addition of sulphite to the vinyl linkage (Fig. S18, ESI[†]). Additionally, a new signal appears around 5.25 ppm, which corresponds to the proton linked to the carbon atom with an attached sulphite group. This large downfield shift (from 7.96 to 5.24 ppm) is mostly caused by the change of hybridization of the carbon atom from sp² to sp³. As the solubility of the **4a**-sulphite adduct was very low, the quality of the ¹H NMR spectrum is also diminished. To obtain more clear results, a model compound was prepared (Fig. S19 and the following synthetic procedure, ESI[†]). The addition of sulphite



Scheme 2 A mechanism of sulphite-**4b** interaction.

was repeated with a model molecule (much better soluble in D₂O/DMSO-*d*₆ mixture). The ¹H NMR spectra of the model and model-sulphite adduct are compared in Fig. S20 (ESI[†]). Additionally, the ¹³C NMR spectrum of the model is depicted in Fig. S21 (ESI[†]). Finally, the formation of the **4b**-SO₃^{2−} (or **4a**-SO₃^{2−}) adduct was confirmed by HRMS measurements where a peak at *m/z* = 540.1057 (580.7468) corresponds to [**4b**-SO₃][−] ([**4a**-SO₃ + 2Na]⁺) (see Fig. S22 and S23, ESI[†]). The adduct was received in two separate and independent reactions: the studied probes and sulphite or bisulphite. In both cases, the same product was obtained which was corroborated by the same MS peak position corresponding only to the adduct with sulphite. Based on the spectroscopic measurements, the following mechanism of the Michael reaction between the investigated probes and sulphite (or bisulfite) was proposed and presented in Scheme 2.

3.6. Limit of detection in DMF/buffer solution (pH = 8)

The detection limit was established by taking advantage of the fluorescence intensity changes induced by the presence of different analyte concentrations. The obtained calibration curves with fitted parameters are presented in Fig. 6 (inset) and the sulphite

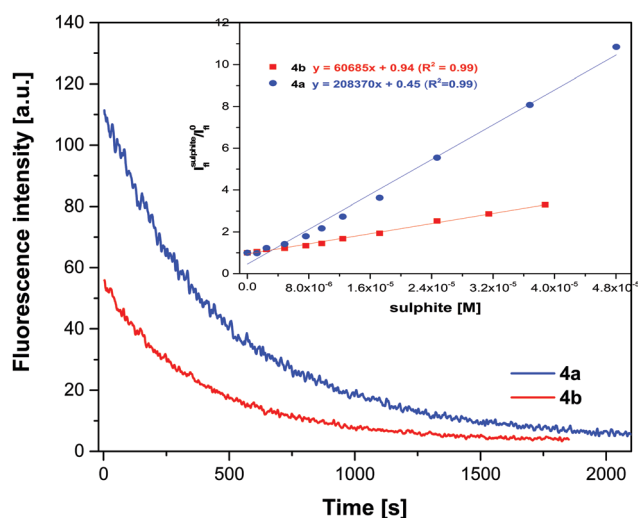


Fig. 6 The kinetics of the analyte addition monitored at 587 nm (**4a**) and 605 nm (**4b**) in the presence of 45 equivalents of sulphite. Inset: The calibration curves prepared on the basis of fluorescence intensity changes recorded at 475 nm (**4a**) and 478 nm (**4b**).

concentration dependent fluorescence spectra are gathered in Fig. S24 (ESI†). Using the value of standard deviation of the intercept (0.48 (**4a**), and 0.089 (**4b**)) and the slope of the calibration line depicted in Fig. 6, the detection limit of sulphite was determined as: 7.56 μM for **4a**, and 4.87 μM for **4b**. The yielded values are satisfactory, especially in terms of WHO sulphite standard in water based flavoured drinks (maximum permitted level 1420 μM)³⁶ which is significantly higher than our detection limit. In the European Union, the maximum permitted sulphite level in final food products is 2 mg kg⁻¹.³⁷ The obtained detection limit is compared to recently investigated probes (Table S1 in the ESI†).^{38–42}

3.7. Response time in DMF/buffer solution (pH = 8)

In order to evaluate the kinetics of the analyte binding, time-dependent fluorescence intensity changes were monitored at 587 nm (**4a**) and 605 nm (**4b**) in the presence of 45 equivalents of sulphite (Fig. 6). It is worth emphasizing that the application of smaller amounts of equivalents is also possible, however, the responsiveness is respectively slower. Assuming that the applied analyte is in excess, the Michael reaction addition follows a pseudo-first order kinetics. The time-dependent changes of the substrate concentration can be described by the expression:

$$[A] = [A_0]e^{-k[B_0]t} \quad (2)$$

where A refers to the investigated probe, and B defines the analyte; $[A]$ – the concentration of A at time t ; $[A_0]$ – the initial concentration of A ; $[B_0]$ – the initial concentration of B ; k is the pseudo-1st-order reaction rate constant.

The fitting of eqn (2) to the fluorescence decay of the substrate yielded a reaction rate constant of: **4b** + sulphite: $k_{4b} = 20.7 \text{ M}^{-1} \text{ s}^{-1}$, **4a** + sulphite: $k_{4a} = 17.4 \text{ M}^{-1} \text{ s}^{-1}$. The experiment showed that the Michael addition reaction of sulphite is within 9 min (**4b**) and 11 min. (**4a**), which indicates that the probes have rapid detection ability to sulphite. Finally, it should be emphasized that the sulphite detection limit of the studied probes is comparable to that obtained for a recently published pyrene based sensor, whereas the kinetics of sulphite addition is much faster (20 min in the presence of 500 equivalents).²⁰

Summing up the photophysical behaviour of the investigated probes, one can conclude that the introduction of a thiophene end group improved the LOD by 1.5 times and accelerated the kinetics of Michael addition by 1.2 times as compared to the probe ended with phenyl. This may be a consequence of larger polarization of the double bond induced by the presence of a better electron acceptor (thiophene group) which, in turn, allows faster nucleophilic attack. Although the fluorescence enhancement recorded for **4b**-sulphite is smaller than for **4a**, it seems, however, that the optical signal is more stable in the presence of competitive anions (see Fig. 4). Nevertheless, in both cases glutathione may interfere with fluorescence readings and result in artificial decreases of sulphite concentration in a real sample.

Table 2 Determination of sulphite in Vistula river water samples

Sample	SO ₃ ²⁻ added (μM)	SO ₃ ²⁻ found (μM)	Recovery (%)
4b	9.69	8.67	90
	17.2	16.4	95
4a	19.8	31.5	159.3

3.8. Real sample applications

The practical utility of the sensors used in this study has been tested in the determination of SO₃²⁻ in Vistula river water samples. The Vistula water sample was found to be free from sulphite, so the sample was prepared by adding a known amount of sulphite to the sample and compared with the same amount dissolved in deionised water. The amounts of added salt and recovery yields are listed in Table 2.

As it was shown in Table 2, compound **4b** was able to measure the concentration of spiked sulphite with good recovery, suggesting that the probe can be applied for detecting sulphite in real samples. In contrast, **4a** cannot be used in environmental applications. The compound **4a** turned out to be not selective enough in river water sample solutions. The found amount of sulphite was twice as high as the real one. It is very likely that, in the river sample solution, **4a** may interact with another species for which compound **4b** is resistant.

Additionally, the practical application of the studied probes for sulphite detection was demonstrated by means of a paper test strip system and shown in Fig. 7. After dipping the probe-stained paper into the solution of sulphite, the paper discoloured (photographs at the top of Fig. 7) and the emission changed from orange or yellow to blue (photographs at the bottom of Fig. 7). Although HSO₃⁻ also caused a colour change, it could be easily distinguished by the naked eye. This experiment is in line

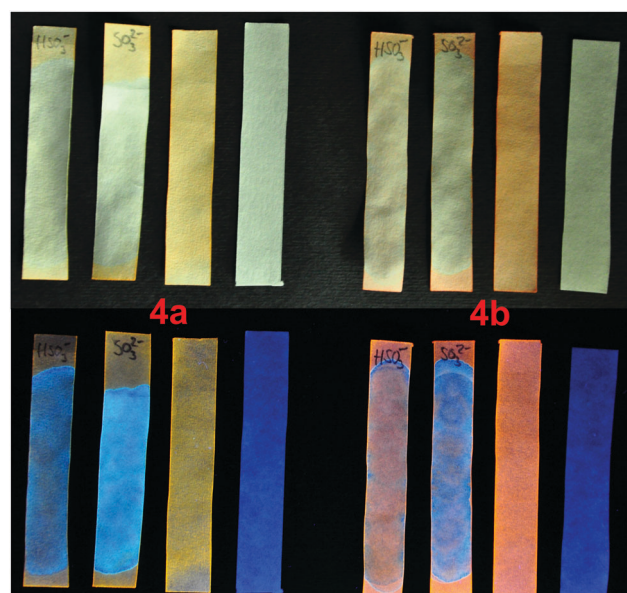


Fig. 7 Photographs of the test paper exposed to various species in the absence (top) and presence (bottom) of UV light (365 nm); from the left: HSO₃⁻, SO₃²⁻, probe alone, and paper without the probe.

with the previous ones (pH dependent effect of sulphite–probe interaction and selectivity studies) confirming an increased sensitivity of the probes to sulphite compared to the bisulphite anion.

4. Conclusions

In summary, we have demonstrated two OFF–ON ratiometric pyrazoline-based sensors which are able to detect sulphite anions. The compounds exhibit weak charge transfer fluorescence which is blocked after the sulphite attachment to the α,β -unsaturated ketone part. As a result, a blue-shift of the absorption and emission spectra of the probes was observed, corresponding to an obvious colour change from orange to colourless which can be noticed by the naked eye. The detection limit of the studied indicators is comparable to that of a recently published pyrene based sensor, while the response speed is twice as fast at a smaller concentration of sulphite. These two parameters can be easily tuned by the introduction of a better acceptor (end group). Here, a simple replacement of phenyl to thiophene improved the response time by 1.2 times and the LOD by 1.5 times. We believe that further increase of the electron acceptor abilities of the end group will lead to higher polarization of the double bond system and faster optical response. Finally, our studies revealed that only **4b** can detect sulphite anions with a good selectivity and sensitivity in environmental samples.

Conflicts of interest

There are no conflicts to declare.

Acknowledgements

This work was performed with equipment purchased thanks to the financial support of the European Regional Development Fund in the framework of the Polish Innovation Economy Operational Program (contract no. POIG.02.01.00-12-023/08). Quantum chemical calculations were carried out in the Academic Computer Center “Cyfronet” in Kraków, Poland. This research was supported in part by PL-Grid Infrastructure. Chemicals for the purpose of the research were financed by the Ministry of Science and Higher Education of the Republic of Poland (DS 3711/ICCh/2017). The authors would also like to acknowledge financial support of TEAM programme (grant number: TEAM/2016-1/9) of the Foundation for Polish Science co-financed by the European Union under the European Regional Development Fund.

References

- C. Ribbe, *Napoleon's Crimes: A Blueprint for Hitler*, Oneworld Publications, 2008.
- Y.-C. Hong, J.-T. Lee, H. Kim, E.-H. Ha, J. Schwartz and D. C. Christiani, *Environ. Health Perspect.*, 2002, **110**, 187–191.
- N. Sang, Y. Yun, H. Li, L. Hou, M. Han and G. Li, *Toxicol. Sci.*, 2010, **114**, 226–236.
- P.-J. Gauthier, O. Sigmarsson, M. Gouhier, B. Haddadi and S. Moune, *J. Geophys. Res.: Solid Earth*, 2016, **121**, 1610–1630.
- E. Rencüzoğullari, H. B. İla, A. Kayraldiz and M. Topaktaş, *Mutat. Res.*, 2001, **490**, 107–112.
- S. H. Mudd, F. Irreverre and L. Laster, *Science*, 1967, **156**, 1599–1602.
- W.-H. Tan, F. S. Eichler, S. Hoda, M. S. Lee, H. Baris, C. A. Hanley, P. E. Grant, K. S. Krishnamoorthy and V. E. Shih, *Pediatrics*, 2005, **116**, 757–766.
- C. Wang, S. Feng, L. Wu, S. Yan, C. Zhong, P. Guo, R. Huang, X. Weng and X. Zhou, *Sens. Actuators, B*, 2014, **190**, 792–799.
- X. Cheng, H. Jia, J. Feng, J. Qin and Z. Li, *J. Mater. Chem. B*, 2013, **1**, 4110–4114.
- K. Rurack, A. Danel, K. Rotkiewicz, D. Grabka, M. Spieles and W. Rettig, *Org. Lett.*, 2002, **4**, 4647–4650.
- M. Mac, T. Uchacz, A. Danel and H. Musiolik, *J. Fluoresc.*, 2013, **23**, 1207–1215.
- M. Mac, T. Uchacz, T. Wróbel, A. Danel and E. Kulig, *J. Fluoresc.*, 2010, **20**, 525–532.
- M. Mac, T. Uchacz, A. Danel, K. Danel, P. Kolek and E. Kulig, *J. Fluoresc.*, 2011, **21**, 375–383.
- P. Wang, N. Onozawa-Komatsuzaki, Y. Himeda, H. Sugihara, H. Arakawa and K. Kasuga, *Tetrahedron Lett.*, 2001, **42**, 9199–9201.
- H.-B. Shi, S.-J. Ji and B. Bian, *Dyes Pigm.*, 2007, **73**, 394–396.
- X. Dai, T. Zhang, Y.-Z. Liu, T. Yan, Y. Li, J.-Y. Miao and B.-X. Zhao, *Sens. Actuators, B*, 2015, **207**, 872–877.
- X. Dai, T. Zhang, J.-Y. Miao and B.-X. Zhao, *Sens. Actuators, B*, 2016, **223**, 274–279.
- T. Haiyu, Q. Junhong, S. Qian, B. Hongyan and Z. Weibing, *Anal. Chim. Acta*, 2013, **788**, 165–170.
- Y.-Q. Sun, P. Wang, J. Liu, J. Zhang and W. Guo, *Analyst*, 2012, **137**, 3430–3433.
- G. Xu, H. Wu, X. Liu, R. Feng and Z. Liu, *Dyes Pigm.*, 2015, **120**, 322–327.
- J. Shen and R. D. Snook, *Chem. Phys. Lett.*, 1989, **155**, 583–586.
- J.-T. Li, X.-H. Zhang and Z.-P. Lin, *Beilstein J. Org. Chem.*, 2007, **3**, art. No13.
- L. A. Kutulya, A. E. Shevchenko and Y. N. Surov, *Chem. Heterocycl. Compd.*, 1975, **11**, 215–217.
- K. Drauz, A. Kleeman and E. Wolfheuss, *US Pat.*, 4.716.237, 1987.
- W. Kohn and L. J. Sham, *Phys. Rev.*, 1965, **140**, A1133–A1138.
- R. G. Parr and W. Yang, *Density-Functional Theory of Atoms and Molecules*, Oxford University Press, Oxford, 1988 (and references therein).
- M. J. Frisch, G. W. Trucks, H. B. Schlegel, G. E. Scuseria, M. A. Robb, J. R. Cheeseman, G. Scalmani, V. Barone, B. Mennucci, G. A. Petersson, H. Nakatsuji, M. Caricato, X. Li, H. P. Hratchian, A. F. Izmaylov, J. Bloino, G. Zheng, J. L. Sonnenberg, M. Hada, M. Ehara, K. Toyota, R. Fukuda, J. Hasegawa, M. Ishida, T. Nakajima, Y. Honda, O. Kitao, H. Nakai, T. Vreven, J. A. Montgomery Jr., J. E. Peralta,

- F. Ogliaro, M. Bearpark, J. J. Heyd, E. Brothers, K. N. Kudin, V. N. Staroverov, R. Kobayashi, J. Normand, K. Raghavachari, A. Rendell, J. C. Burant, S. S. Iyengar, J. Tomasi, M. Cossi, N. Rega, J. M. Millam, M. Klene, J. E. Knox, J. B. Cross, V. Bakken, C. Adamo, J. Jaramillo, R. Gomperts, R. E. Stratmann, O. Yazyev, A. J. Austin, R. Cammi, C. Pomelli, J. W. Ochterski, R. L. Martin, K. Morokuma, V. G. Zakrzewski, G. A. Voth, P. Salvador, J. J. Dannenberg, S. Dapprich, A. D. Daniels, Ö. Farkas, J. B. Foresman, J. V. Ortiz, J. Cioslowski and D. J. Fox, *Gaussian 09, Revision A.1*, Gaussian, Inc., Wallingford, CT, 2009.
- 28 A. D. Becke, *Phys. Rev. A: At., Mol., Opt. Phys.*, 1988, **38**, 3098–3100.
- 29 C. Lee, W. Yang and R. G. Parr, *Phys. Rev. B: Condens. Matter Mater. Phys.*, 1988, **37**, 785–789.
- 30 S. Miertuš, E. Scrocco and J. Tomasi, *Chem. Phys.*, 1981, **55**, 117–129.
- 31 S. Miertuš and J. Tomasi, *Chem. Phys.*, 1982, **65**, 239–245.
- 32 M. Montalti, A. Credi, L. Prodi and M. T. Gandolfi, *Handbook of Photochemistry*, Taylor & Francis Group, LLC, 3rd edn, 2006.
- 33 M. R. V. Sahyun, G. P. Crooks and D. K. Sharma, *Proc. SPIE*, 1991, 1436, 125–133.
- 34 K. Rurack, J. L. Bricks, B. Schulz, M. Maus, G. Reck and U. Resch-Genger, *J. Phys. Chem. A*, 2000, **104**, 6171–6188.
- 35 D. A. Keller and D. B. Menzel, *Chem.-Biol. Interact.*, 1989, **70**, 145–156.
- 36 National coordinated survey of sulphite levels in sausages, cordial and dried fruit, <http://www.foodstandards.gov.au/science/surveillance/documents/Sulphites%20survey.pdf>.
- 37 Commission Regulation (EU) no. 1130/2011, 11 November 2011.
- 38 S. Samanta, P. Dey, A. Ramesh and G. Das, *Chem. Commun.*, 2016, **52**, 10381–10384.
- 39 Q. Sun, W. B. Zhang and J. H. Qian, *Talanta*, 2017, **162**, 107–113.
- 40 J. B. Chao, Y. H. Liu and Y. Zhang, *Spectrochim. Acta, Part A*, 2015, **146**, 33–37.
- 41 M. Gómez, E. G. Perez, V. Arancibia, C. Iribarren, C. Bravo-Díaz, O. García-Beltrán and M. E. Aliaga, *Sens. Actuators, B*, 2017, **238**, 578–587.
- 42 G. Wang, H. Chen, X. L. Chen and Y. M. Xie, *RSC Adv.*, 2016, **6**, 18662–18666.